1 **Title**

2 Bread feeding is a robust and more physiological enteropathogen administration method
3 compared to oral gavage

4

5 **Authors**

6 Anne Derbise[1]*, Hebert Echenique-Rivera [1], Marta Garcia-Lopez [1], Rémi Beau [1], Myriam
7 Mattei[2], Petra Dersch [3] and Javier Pizarro-Cerdá[1]*

8 1 Yersinia Research Unit, Institut Pasteur, Paris, France

9 2 Animalerie Centrale, Centre de ressources et recherches animales, Institut Pasteur, Paris,
10 France

11 3 Institute of Infectiology, Center for Molecular Biology of Inflammation, University of
12 Münster, Münster, Germany

13 * co-corresponding authors

14

15 **running title**

16 bread feeding to study entheropathogens

17 **key words**

18 oral infection, pathogenesis, bread feeding, *Yersinia pseudotuberculosis*

19

Abstract

Oral administration is a preferred model for studying infection by bacterial enteropathogens such as *Yersinia*. In the mouse model, the most frequent method for oral infection consists of oral gavage with a feeding needle directly introduced in the animal stomach via the esophagus. In this study, we compared needle gavage to bread feeding as an alternative mode of bacterial administration. Using a bioluminescence-expressing strain of *Yersinia pseudotuberculosis*, we detected very early upon needle gavage a bioluminescent signal in the neck area together with a signal in the abdominal region, highlighting the presence of two independent sites of bacterial colonization and multiplication. Bacteria were often detected in the esophagus and trachea, as well as in the lymph nodes draining the salivary glands, suggesting that lesions made during needle introduction into the animal oral cavity lead to rapid bacterial draining to proximal lymph nodes. We then tested an alternative mode of bacterial administration using small pieces of white bread containing bacteria. Upon bread feeding infection, mice exhibited a stronger bioluminescent signal in the abdominal region as compared to needle gavage, and no signal was detected in the neck area. Moreover, *Y. pseudotuberculosis* incorporated in the bread is less susceptible to the acidic environment of the stomach and is therefore more efficient in causing intestinal infections. Based on our observations, bread feeding constitutes a natural and more efficient administration method which does not require specialized skills, is less traumatic for the animal, and results in diseases that more closely mimic food-borne intestinal infection.

Introduction

Animal infection models represent major research tools to understand human disease, as they allow to investigate in a relevant physiological environment the very complex interactions that take place between pathogens and hosts during organ/tissue colonization or whole-body dissemination (1, 2). For the study of bacterial enteropathogens, oral administration is a preferred infection route to assess intestinal colonization and pathogenesis in mammalian hosts. The most often used methodology for oral infection in laboratories using mice as models consists of oral gavage with a feeding needle introduced in the stomach via the esophagus. However, several laboratories have reported, using bioluminescence-expressing pathogens, colonization in sites distant from the abdominal region after orogastric infection, suggesting abrasions in the laryngopharynx region (3-6). Although, the impact of such accidental colonization on the overall infectious process is not known, we cannot exclude the possibility of bacterial dissemination in the bloodstream independently to the intestinal infection. In order to avoid this potential problem, alternative modes of pathogen administration have been described, such as bread feeding (7, 8) or drinking water delivery (9, 10).

Enteropathogenic *Yersinia* are the third bacterial cause of human gastrointestinal infections in Europe (11). Although much less often isolated than *Y. enterocolitica*, *Y. pseudotuberculosis* is responsible for acute gastroenteritis and mesenteric lymphadenitis in a wide variety of animals including rodents, domestics animals, non-human primates and humans (12). After oral ingestion, *Y. pseudotuberculosis* localizes to the ileum and proximal colon and can pass/cross the intestinal barrier, invading its host through gut-associated lymphoid tissues and Peyer's patches (13). In humans, dissemination to deeper tissues and the bloodstream are frequent in patients with underlying disease conditions (such as diabetes mellitus, liver

cirrhosis, and hemochromatosis) and can lead to septicemia as a severe outcome of the infection (14) (15).

While performing mice oral administration of *Y. pseudotuberculosis* with a feeding needle, we regularly noticed that some animals exhibit spleen infections without displaying the presence of bacteria in Peyer's patches (PPs) or mesenteric lymph nodes (MLNs), suggesting the passage of bacteria in the blood stream independently of the colonization of the gut-associated lymphoid tissues (data not shown). Since it has been reported that needle gavage can cause lesions in the oropharyngeal region (3), we decided to re-examine this mode of administration and compare it to an alternative administration method (bread feeding) with a fully virulent *Y. pseudotuberculosis* strain expressing bioluminescence in order to follow bacterial dissemination over time in the whole animal body. Our results clearly illustrate that needle feeding promotes *Y. pseudotuberculosis* colonization not only of the intestinal tract but also the neck region with a tropism for salivary glands lymph nodes. On the contrary, bread feeding induces a much more robust intestinal tract infection that is never associated to neck region infections. Moreover, bread feeding allows to protect bacteria from the acidic environment of the stomach. We conclude therefore that bread feeding is a better oral administration route to investigate the pathophysiology of bacterial enteropathogen infection.

Results

Construction of a constitutively bioluminescent *Y. pseudotuberculosis* strain

The IP32953 *Y. pseudotuberculosis* strain, isolated from the stools of a human patient, was chosen for this study due to its capacity to express two major virulence factors, the type 3 secretion system (T3SS) and the Yersiniabactin (Ybt) iron uptake machinery. This strain has been previously shown to be fully virulent in laboratory mice (16) (17).

To perform a comparative analysis of bacterial dissemination *in vivo* after oral infection, the strain IP32953 was genetically engineered to constitutively express bioluminescence. In order to correlate bioluminescence to bacterial numbers during animal infection, the *luxCDABE* operon (placed under the control of the constitutive *rplN* promoter) was stably introduced into the *Y. pseudotuberculosis* chromosome using the mini-Tn7-transposon technology (18, 19). The resulting strain, IP32953-lux, harbors the construct *mini-Tn7-Km-*P_{rplN}*-luxCDABE* between the two housekeeping genes *glmS* and *pstS* (**Fig. S1A**)(19). Stability of the bioluminescence signal over time was determined by performing 10 subcultures of IP32953-*lux* in LB without antibiotics over 17 days. At different time points, bacterial aliquots were streaked on LB plates and individual colonies were checked for their capacity to emit bioluminescence. After 10 subcultures, 100% of the CFU expressed bioluminescence confirming the stability of the bioluminescent phenotype in the bacterial population (data not shown).

Strain IP32953-*lux* displayed similar *in vitro* growth and virulence as the parental wild type IP32953 strain (data not shown). Therefore, IP32953-*lux* was used to determine the characteristics and relevant differences between the two infection methods applied: oral gavage with a feeding needle versus bread feeding.

Y. pseudotuberculosis colonizes the neck and the abdominal region of infected animals upon needle feeding

We first set up the bread feeding protocol in OF1 mice based on a previously reported methodology (7). In our study, instead of using melted butter as a vehicle to deliver bacteria and to attract mice to bread, mice were first trained to feed on bread only (see Materials & Methods) and then were infected with bread supplemented with a bacterial suspension in PBS. A pilot experiment using this new method allowed us to validate that within less than 5 min

mice consumed bread supplemented with 8E7 IP32953-*lux* CFUs, subsequently exhibiting bioluminescence in the PPs and MLNs, confirming therefore *Y. pseudotuberculosis* colonization and dissemination in the intestinal tract as expected for an enteropathogen **(Fig. S1B).**

We then proceed to compare needle versus bread feeding as oral administration routes. 24 h after oral administration of 3.5E8 IP32953-*lux* CFUs, mice were monitored for bioluminescence and regions of interest (ROI) were identified for bioluminescence imaging (BLI) measurements. Upon needle gavage, up to 80% of the mice displayed a BLI signal in two distinct regions of the body, one in the expected abdominal region and a second in the neck, whereas upon bread feeding none of the mice exhibited a neck signal and bioluminescence was restricted to the abdomen (**Fig. 1A**). ROI measurements in the neck region of needle-infected mice indicate that the level of BLI is similar to the one coming from the abdominal region, suggesting that bacteria colonize, disseminate and multiply in the neck as efficiently as in the abdomen (**Fig. 1B**). This comparative analysis indicates that oral administration of *Y. pseudotuberculosis* using needle feeding results in infection of the neck region, a phenotype that is not observed upon bread feeding.

Upon needle feeding, *Y. pseudotuberculosis* multiplies in the intersection of the oesophagus and trachea and disseminates to the draining lymph nodes of the submandibular area

To identify which specific neck region is colonized by *Y. pseudotuberculosis*, mice were first orally gavaged with 4E8 IP32953-*lux* CFUs; then at 24 and 48 h post infection, mice exhibiting a BLI signal in the neck were euthanized and dissected in the cervical ventral region (see Materials & Methods)**.** After skin removal, all the mice exhibited a BLI signal coming from the cervical soft tissue composed of salivary glands, lymph nodes (LNs) and

adipose tissues (**Fig. 2**). Among 10 dissected mice, nine exhibited bioluminescent signals in LNs from the salivary glands region (**Fig. 2A, 2C$_1$, 2D$_1$**). Although there was no preferential right or left LN colonization, we often noticed that after removal of a first LN producing high amounts of photons, it was possible to identify secondary LNs producing less light, indicating variable levels of bacterial colonization among LNs. Each time a BLI positive LN was isolated, we verified its bacterial content by homogenization and CFU counting on agar plates (**Fig. 2C$_1$, 2D$_1$**). In addition to LNs, we noticed in 70% of the mice a strong BLI signal in the esophagus and/or trachea (**Fig. 2B, 2C**). Dissection of the esophagus and trachea sections associated with BLI allowed us to localize bacterial colonization at the junction of these two structures (**Fig. 2C$_2$**), suggesting a probable deposition of bacteria in the tissue consecutive to the introduction of the needle in the esophagus. Finally, half of the mice emitted a BLI signal in the oral cavity corresponding most of the time to the skin associated to the lip (**Fig. 2D, 2D$_2$**). From these results, we speculate that the use of a feeding needle entails a risk of creating lesions in the skin of the mouth as well as in the tissue at the junction of the esophagus and trachea, from which *Y. pseudotuberculosis* can disseminate to and multiply in the draining LNs located in the salivary glands region.

Although we do not know the impact of the *Y. pseudotuberculosis* neck colonization in the overall infectious process, we cannot exclude the possibility of bacterial dissemination in the blood stream occurring independently to the intestinal colonization and translocation at the gastro-intestinal barrier.

Bread feeding protects *Y. pseudotuberculosis* from the acidic gastric environment and promotes efficient intestinal colonization

We next compared the kinetics of bacterial dissemination upon bread feeding versus needle feeding. Mice were orally infected with 3.5E8 IP32953-*lux* CFUs and imaged at 0.5, 6, 24, 48

and 72 h post infection (**Fig. 3)**. At each time point, photon emission was measured from the abdominal region and neck region. As indicated in **Fig. 3A** and **3B,** upon bread feeding the BLI signal in the abdominal region is detected as early as 30 min post infection, then decreases to an almost undetectable signal at 6 h p.i., and in a second phase increases continuously. Upon needle feeding the BLI signal is barely detectable before 24 h p.i.: after that time point, the BLI signal is detected in the neck **(Fig 3A, 3D)** and the abdominal region **(Fig. 3A, 3B)** where it continuously increases over time. It is noteworthy that the neck region signal was never detected in bread-infected animals **(Fig. 3D)** even at later time points (data not shown). Statistical analysis indicates a significantly higher light emission signal in the abdominal region at early (0.5 h) and later time points (72 h) when using bread compared to needle **(Fig. 3B).** This observation correlates with the lower amount of *Y. pseudotuberculosis* found in the feces six hours post needle feeding as shown by CFU counting (**Fig. 3C**), suggesting a lower number of bacteria surviving the passage through the stomach.

When needle feeding is used, bacteria are delivered directly to the stomach, a compartment known to have an acidic pH aggressive for microorganisms. To evaluate whether the lower amount of light observed in the abdominal region of needle-infected mice was due to bacterial killing by the acidity of the stomach, we infected animals using the needle with either bacteria resuspended in PBS only, or in PBS buffered with $CaCO_3$ (20). As shown in **Fig. 4A** and **4B**, buffering the bacterial inoculating medium significantly increases the BLI signal in the abdominal region of infected mice as well as the amount of bacterial CFUs recovered in the feces (**Fig. 4C**). Our results therefore indicate that bacterial bread delivery protects *Y. pseudotuberculosis* from the acidic gastric environment and promotes efficient intestinal colonization.

Mice are more susceptible to *Y. pseudotuberculosis* infection when administered via bread feeding

The better survival of *Y. pseudotuberculosis* when associated with $CaCO_3$ prior to needle feeding led us to evaluate whether it would change the overall lethal dose 50 (LD_{50}) of strain IP32953-*lux* when administered with bread. Thus, mice were infected using three conditions (needle with or without supplementation of $CaCO_3$, and bread) with four different *Y. pseudotuberculosis* IP32953-*lux* concentrations (2.5E5, 2.5E6, 2.5E7, and 2.5E8 CFU). Animals were monitored over time for BLI imaging (**Fig. 5 and 6**), body weight loss (**Fig. 5B, 6B**), signs of disease, and lethality to allow measurements of LD_{50} (**Fig. 7**).

The use of the needle without supplementation of $CaCO_3$ gave the highest LD_{50} (5.2E6 CFU)(**Fig. 7C**). When bacteria are mixed with $CaCO_3$, the LD_{50} is lower (1.8E6 CFU) suggesting a beneficial effect of $CaCO_3$ when the needle feeding administration is used (**Fig. 7B**). However, the lowest calculated LD_{50} was obtained when OF1 mice were bread-infected (LD_{50}=9.5E5) (**Fig. 7A**). The BLI and weight loss illustrate very well the differences of bacterial dissemination and multiplication at a low dose (2.5E5 IP32953-*lux* CFUs) between the three infection conditions (**Fig. 5A, 5B**). At this low dose, none of the mice treated with the needle (without supplementation of $CaCO_3$) showed signs of disease or weight loss while the mice treated with bread or needle supplemented with $CaCO_3$ showed signs of disease, weight loss and mortality (30 to 40% of them died) **(Fig. 5B, 5C).** When the same parameters are monitored after oral infection with a higher dose (2.5E7 IP32953-*lux* CFUs) no significant differences were observed between the 3 conditions of administration, as shown in **(Fig. 6A, 5B, 5C**). It is noteworthy that even at low bacterial concentrations (2.5E5 CFU), needle feeding (with or without $CaCO_3$) leads to neck colonization, whereas none of the mice showed a neck BLI signal upon bread feeding (**Fig. 5A**). Our results therefore show that

213 infection using bread feeding is more efficient for *Y. pseudotuberculosis* delivery to the
214 intestinal tract, resulting in better colonization even at low inoculum concentrations.
215
216 **Discussion**
217 When studying host pathogen interactions, the choice of a laboratory experimental model of
218 infection is crucial. Besides the choice of the animal species and the pathogen to study,
219 important parameters that have to be taken into account include the control of the dose of the
220 infectious agent administered to each animal, the rapidity to handle the animal and the stress
221 induced by the animal manipulation. For decades, laboratories interested in studying animal
222 oral infection have used needle feeding to orally deliver infectious agents. Although needle
223 feeding allows to control the delivered dose, there are drawbacks such as the requirement of a
224 specific manipulator training, the use of anesthesia when animals are particularly agitated, or
225 the stress induced by the handling of the animal. Importantly, in this study we show that the
226 use of needle gavage induces damage to the oral cavity of infected animals, leading to
227 pathogen colonization in tissues and organs distant from the intestinal tract. Although it is not
228 known whether such artificial colonization affects the intestinal infection process, it is
229 reasonable to question its impact on the overall host immune response.
230 In order to avoid this potentially unwanted response, we propose the use of a bread feeding
231 methodology which allows a non-traumatic pathogen administration, where animal handling
232 is minimized and therefore is less stressful for both the manipulator and the animal. We found
233 that the habituation step to feed on bread few days prior to the infection is crucial for effective
234 bread feeding, with no need of additional melted butter as a vehicle as proposed by others (7)
235 (8).
236 Bread feeding constitutes a very good administration method since it allows a control of the
237 dose administered and is a fast procedure where all bread is generally consumed by mice in

less than 5 minutes as opposed to the drinking water method (within several hours) described by others (10).

In addition, our study shows that *Y. pseudotuberculosis* colonizes better the intestinal tract when administered with bread compared to the needle, with no need to buffer the bacterial cell suspension. The differences in LD_{50} measurement obtained in our study using the same *Y. pseudotuberculosis* virulent strain but different administration protocols encourage us to reinvestigate the infectious process by *Y. pseudotuberculosis* after bread feeding delivery. Finally, we expect that this delivery method can be extended to other studies of host pathogen interactions with different intestinal pathogens.

Materials and Methods

Culture conditions and bacterial strain construction

Bacteria were grown at 28°C in lysogeny broth (LB) or on LB agar (LBA) plates. Bacterial concentrations were evaluated by spectrometry at 600 nm and plating on LBA. Kanamycin (Km, 30 µg/ml), or irgasan (0.1 µg/ml) were added to the media when necessary.

The fully virulent IP32953, serotype 1b *Y. pseudotuberculosis* isolated from a human stool in France, was used as parental strain to generate IP32953-*lux*, a bioluminescence expressing strain. As previously described (19) the *Photorabdus luminescence lux CDABE* operon controlled by the *rplN* constitutive *Yersinia* promoter was introduced into IP32953 chromosome via the Tn*7* technology (18). Plasmid pUCR6K-mini-Tn*7*-*Km*^{r}-*luxCDABE* and the transposase-encoding plasmid pTNS2 were co-electroporated to IP32953 electrocompetent cells. Bioluminescent recombinant clones were selected on LB agar plates supplemented with Km. The recombinant *Y. pseudotuberculosis* IP32953-*lux* was verified (i) for Tn7-P*rplN*-lux chromosomal insertion by PCR using primers flanking the Tn*7* insertion site, P*glmS* 5′-gctatacgtgtttgctgatcaagatg-3′, P*pstS* 5′- acgccaccggaagaaccgatacct-3′, PTn*7*L 5′-

263 attagcttacgacgctacaccc-3′, and PTn*7*R 5′- cacagcataactggactgatttc-3′, (ii) for similar growth
264 rate as the parental strain in LB, and (iii) for similar virulence via oral route using the needle
265 feeding administration. Stability of the *lux* operon was verified by successive subcultures in
266 LB without antibiotic pressure and measurements of BLI signal on CFU resuspended in 0.1
267 mL LB using a Xenius 96 well plate reader (SAFAS Monaco).
268
269 **Ethics statement**
270 Animals were housed in the Institut Pasteur animal facility accredited by the French Ministry
271 of Agriculture to perform experiments on live mice (accreditation B 75 15-01, issued on May
272 22, 2008), in compliance with French and European regulations on the care and protection of
273 laboratory animals (EC Directive 86/609, French Law 2001-486 issued on June 6, 2001). The
274 research protocol was approved by the French Ministry of Research (N° CETEA 2014-0025)
275 and Institut Pasteur CHSCT (n°0399).
276
277 **Animal experiments**
278 Female 7-week-old OF1 mice were purchased from Charles River France and allowed to
279 acclimate for 1 week before infection. Prior to infection mice were fasted 16 h and had
280 continuous access to water. All oral infections were performed on non-anesthetized animals.
281 Serial dilution of bacterial suspension was performed in Phosphate-buffered saline (PBS
282 without $CaCl_2$/MgCl2) from cultures grown for 48 h at 28°C in LB agar plates.
283 For oral gavage mice were administered a 0.2 mL bacterial suspension using an animal
284 feeding stainless steel bulbous-ended needle (0.9 mm × 38 mm, 20G × 1.5″, Cadence Science
285 cat. no. 9921). The bulbous-ended needle was inserted over the tongue into the esophagus and
286 stomach as previously described (20). When required, the 0.2 ml bacterial suspension used for
287 oral gavage (feeding needle) was mixed with 0.3 ml of a 50-mg ml^{-1} suspension of $CaCO_3$ in

PBS without $CaCl_2$/$MgCl_2$ and the 0.5 ml mix was administered. Since $CaCO_3$ is not soluble at this concentration the bacterial suspension was mixed to $CaCO_3$ at once before each feeding needle injection.

For bread feeding, mice were first adapted to feed on bread prior to the infection. Thus, three days before infection, the food was replaced by small pieces of white bread (approximately 9 mm^2) to allow mice to feed on bread for a 2 h period. The same bread adaptation was repeated once 24 h before infection. Then 16 h prior to the infection the food was removed, and mice were fasted with access to water. A 20 µL bacterial suspension (without supplementation of $CaCO_3$) was deposited on one piece of bread, placed in an empty and clean cage where one mouse was introduced. Each mouse was visually monitored until complete bread feeding. Generally, bread feeding took from 30 seconds up to 10 minutes per mouse. After feeding animals were housed in a cage with new litter, and access to food and water *ad libitum*.

After infection animals were monitored daily for 21 days and every day the litter was renewed in order to limit accumulation of feces in the cage and avoid cross contamination between mice.

BLI imaging and dissection

In vivo imaging was performed with an In Vivo Imaging System (IVIS 100, Caliper Life Sciences). Animals were anesthetized using a constant flow of 2,5% isoflurane mixed with oxygen. Images were acquired with binning 4 and an exposure time from 10 sec. to 2 min. according to the signal intensity. To quantify luminescence signal, region of interest (ROI) were drawn and measurements of the ROI are given as average radiance (photons/s/cm2/steradian). Uninfected mice were used to set the light emission background.

Analysis of the cervical region was performed sequentially starting by the removal of the skin on euthanized animals and imaging, followed by removal of the most intense bioluminescent

tissue and imaging again of the animal to identify lower intensity signal. When signal was still detected after removal first identified bioluminescent tissue the same sequence was repeated until no signal could be detected. Each organ and tissues were aseptically removed, placed in glass beads containing tubes 0.5 ml PBS and subjected to homogenization to determine bacterial loads. Feces were collected from live mice and were homogenized in PBS using disposable homogenizers (Piston Pellet from Kimble Chase, Fisher Sci.) and serial dilutions were performed to determine bacterial loads.

Statistical analysis

Data were analysed using T test non-parametric Mann-Whitney with the Graph Prism 5.0 software (San Diego, CA, USA). P-values ≤ 0.05 were considered significant.

References

1. Colby LA, Quenee LE, Zitzow LA. 2017. Considerations for Infectious Disease Research Studies Using Animals. Comparative Medicine 67:222-231.
2. Swearengen JR. 2018. Choosing the right animal model for infectious disease research. Animal Model Exp Med 1:100-108.
3. Glomski IJ, Piris-Gimenez A, Huerre M, Mock M, Goossens PL. 2007. Primary involvement of pharynx and peyer's patch in inhalational and intestinal anthrax. PLoS Pathog 3:e76.
4. Boyle JP, Saeij JP, Boothroyd JC. 2007. Toxoplasma gondii: inconsistent dissemination patterns following oral infection in mice. Exp Parasitol 116:302-5.
5. Trcek J, Berschl K, Trulzsch K. 2010. In vivo analysis of Yersinia enterocolitica infection using luxCDABE. FEMS Microbiol Lett 307:201-6.

337 6. Uliczka F, Pisano F, Kochut A, Opitz W, Herbst K, Stolz T, Dersch P. 2011.
338 Monitoring of gene expression in bacteria during infections using an adaptable set of
339 bioluminescent, fluorescent and colorigenic fusion vectors. PLoS One 6:e20425.
340 7. Bou Ghanem EN, Myers-Morales T, D'Orazio SE. 2013. A mouse model of foodborne
341 Listeria monocytogenes infection. Curr Protoc Microbiol 31:9B 3 1-9B 3 16.
342 8. Hooker-Romero D, Schwiesow L, Wei Y, Auerbuch V. 2019. Mouse Models of
343 Yersiniosis. Methods Mol Biol 2010:41-53.
344 9. Fahlgren A, Avican K, Westermark L, Nordfelth R, Fallman M. 2014. Colonization of
345 cecum is important for development of persistent infection by Yersinia
346 pseudotuberculosis. Infect Immun 82:3471-82.
347 10. O'Donnell H, Pham OH, Benoun JM, Ravesloot-Chavez MM, McSorley SJ. 2015.
348 Contaminated water delivery as a simple and effective method of experimental
349 Salmonella infection. Future Microbiol 10:1615-27.
350 11. European Food Safety Authority and European Centre for Disease Prevention and
351 Control. 2018. The European Union summary report on trends and sources of
352 zoonoses, zoonotic agents and food-borne outbreaks in 2017, vol 16.
353 12. Galindo CL, Rosenzweig JA, Kirtley ML, Chopra AK. 2011. Pathogenesis of Y.
354 enterocolitica and Y. pseudotuberculosis in Human Yersiniosis. J Pathog 2011:182051.
355 13. Marra A, Isberg RR. 1997. Invasin-dependent and invasin-independent pathways for
356 translocation of Yersinia pseudotuberculosis across the Peyer's patch intestinal
357 epithelium. Infect Immun 65:3412-21.
358 14. Kaasch AJ, Dinter J, Goeser T, Plum G, Seifert H. 2012. Yersinia pseudotuberculosis
359 bloodstream infection and septic arthritis: case report and review of the literature.
360 Infection 40:185-90.

15. Vincent P, Leclercq A, Martin L, Yersinia Surveillance N, Duez JM, Simonet M, Carniel E. 2008. Sudden onset of pseudotuberculosis in humans, France, 2004-05. Emerg Infect Dis 14:1119-22.

16. Blisnick T, Ave P, Huerre M, Carniel E, Demeure CE. 2008. Oral vaccination against bubonic plague using a live avirulent Yersinia pseudotuberculosis strain. Infect Immun 76:3808-16.

17. Pouillot F, Fayolle C, Carniel E. 2007. A putative DNA adenine methyltransferase is involved in Yersinia pseudotuberculosis pathogenicity. Microbiology 153:2426-34.

18. Choi KH, Gaynor JB, White KG, Lopez C, Bosio CM, Karkhoff-Schweizer RR, Schweizer HP. 2005. A Tn7-based broad-range bacterial cloning and expression system. Nat Methods 2:443-8.

19. Derbise A, Dussurget O, Carniel E, Pizarro-Cerda J. 2019. Real-Time Monitoring of Yersinia pestis Promoter Activity by Bioluminescence Imaging. Methods Mol Biol 2010:85-97.

20. Disson O, Nikitas G, Grayo S, Dussurget O, Cossart P, Lecuit M. 2009. Modeling human listeriosis in natural and genetically engineered animals. Nat Protoc 4:799-810.

21. Reed I, Muench H. 1938. A simple method for estimating fifty percent end points. Am J Hyg; 27:493-497.

Legends

Fig. 1 Comparative bioluminescence imaging of mice infected by either needle or bread feeding.

OF1 mice were infected with 3.5E8 CFUs of *Y. pseudotuberculosis* bioluminescent strain (IP32953-*lux*) using a 20G x 1,5" feeding needle or a piece of bread. (A) At 24 hours (h) post infection mice were imaged using an IVIS Spectrum imaging system with an acquisition time of 2 minutes and small binning. Uninfected mice (UI) were used to set the light emission background. Regions of interest (ROI) were drawn in the neck region (red frame) and the abdominal region (ar, blue frame) using the Living Image 4.5 software. (B) ROI average bioluminescence (photon/sec/cm2/sr) was calculated for each individual mice and data were analyzed using Prism 5.0 software for T test non-parametric Mann Whitney, p>0,05(ns), p<0,0015(**), p<0,0002(***). Median of the values are indicated by an horizontal bar. Bioluminescence signal is detected in the neck of 80% of the needle infected animals with an average radiance not statistically different than the signal from the abdominal region, whereas none of the mice infected with bread presented a signal in the neck. Although the median of the abdominal region is higher when mice are infected with bread, the overall signal is not statistically different due to the variability between mice.

Fig. 2 Mouse regional ventral cervical anatomy and analysis of the site of bacterial colonization after needle feeding.

(A) salivary glands outlined in white doted lines are bilateral located in the cervical neck,

(B) after the salivary glands removal, trachea and underneath esophagus are accessible as schematically indicated.

(C) and (D) Mice exhibiting BLI signal in the neck 24 h or 48 h post-infection (needle feeding with 4E8 CFU of IP32953-*lux*) were euthanized using CO_2 and a dissection procedure

405 associated with BLI acquisition was performed step by step. Two representative mice are
406 shown. After a first step of skin removal, the salivary glands region was dissected and lymph
407 nodes (LN1-4) found in this region were collected. Then the esophagus and trachea section
408 were collected as indicated by the schematized red scissors. Regions of interest (ROI) were
409 drawn and average bioluminescence (photon/sec/cm2/sr) was calculated for each dissected
410 organs. Organs exhibiting BLI signal were homogenized in PBS and enumerated for bacterial
411 count (CFU). Panel C_1: lymph nodes : LN1(ROI=2E5; CFU=2E4), LN2 (ROI=5.4E4;
412 CFU=4E3). Panel C_2: esophagus (ROI=2E6; CFU=4E5) and trachea (ROI=6E6; CFU=6E5).
413 Panel D_1 : lymph nodes LN3 (ROI=2.5E7; CFU=4E6) and LN4 (ROI=1E6; CFU=4E5). Panel
414 D_2: skin from the mouth (ROI=9.3E5; CFU=not done). Among 10 dissected mice, nine
415 exhibited bioluminescent signals in lymph nodes from the salivary glands region (panel C_1
416 and D_1), 7 in the esophagus and/or trachea (panel C_2) and five close to the mouth/lip region
417 (panel D_2).
418
419 **Fig. 3 Comparative analysis of bacterial survival upon bread versus needle feeding**.
420 OF1 mice were infected with 3,5E8 IP32953-*lux Y. pseudotuberculosis* CFUs using bread or
421 feeding needle and at 0.5, 6, 24, 48 and 72 h post infection mice were imaged using an IVIS
422 Spectrum imaging system. (A) Monitoring of 5 representative mice from 0.5 to 48 h post
423 infection using needle and bread feeding, same color scale (min=5E3 max=5E5) with settings
424 2 min time of exposure and small binning. (B) ROI were drawn in the abdominal region and
425 average bioluminescence (photon/sec/cm2/sr) was calculated for each mouse at 0.5, 6, 24, 48
426 and 72 h post infection using bread (red circle) or needle (open circle)**.** (C) Enumeration of *Y.*
427 *pseudotuberculosis* IP32953-*lux* in feces at 0.5, 6, 24, 48 and 72 h post infection using bread
428 (red circle) or needle (open circle) feeding. (D) ROI were drawn in the neck region and
429 average bioluminescence (photon/sec/cm2/sr) was calculated for each mouse at 0.5, 6, 24, 48

and 72 h post infection using bread (red circle) or needle (open circle) feeding**.** Median of the values are indicated by a horizontal bar. Data were analyzed using Prism 5 software for T test non-parametric Mann Whitney, p<0,002 (**); p=0,014(*); ns: not significative p>0,05. The increased BLI signal in the abdominal region and bacterial load in the feces when mice are infected by bread feeding indicates a more efficient delivery of bacteria and colonization of the intestinal tract compared to the needle feeding protocol. BLI signal increases over time in the neck of mice infected with the needle while no signal was detected in the neck of the animals infected with bread.

Fig. 4. Protective effect of $CaCO_3$ when bacteria are administered directly in the stomach by needle feeding.

OF1 mice were infected with 4 to 5E8 *Y. pseudotuberculosis* IP32953-*lux* CFUs using two needle feeding conditions: bacterial suspension in PBS (open circle) or in PBS supplemented with $CaCO_3$ (30 mg/ml) (green circle). At 0.5, 24 and 48 h post infection mice were imaged using an IVIS Spectrum imaging system. (A) A representative panel of the animals for the two conditions are shown using same color scale (min=7E3 max=5E5) with settings 2min time of exposure and small binning. (B) Regions of interest (ROI) were drawn in the abdominal region and average bioluminescence (photon/sec/cm2/sr) was calculated for each mouse. (C) Enumeration of *Y. pseudotuberculosis* IP32953-*lux* in feces at 6, 24, and 48 h post infection. Median of the values are indicated by a horizontal bar. Data were analyzed using Prism 5 software for T test non-parametric Mann Whitney, p<0,0001 (****), p>=0,0001(***); p=0,0014(**). Addition of $CaCO_3$ to the bacterial suspension protects *Y. pseudotuberculosis* when administered via a feeding needle directly in the stomach.

Fig. 5. Comparative analysis of the course of infection using the three protocols of administration with 2.5E5 CFU of *Y. pseudotuberculosis*.

OF1 mice were orally infected with 2.5E5 (A, B, C) *Y. pseudotuberculosis* strain IP32953-*lux* CFUs and monitored overtime for BLI signal, weight loss and mortality after needle feeding of bacteria resuspended in PBS (black line), in PBS supplemented with $CaCO_3$ (green line), or after bread feeding of bacteria resuspended in PBS only (red line).

Quantification of the bioluminescent signal from the abdominal region is shown below the mice pictures in each condition at each time point (24, 48, 72 and 168-192 h p.i.). Red dotted lines indicate the average radiance of ROI measurements above which animals are in terminal illness. Red crosses positioned on the X axis indicate dead mice. Comparative weight loss (B) and survival of mice (C) for 21 days using the three protocols of administration. Bread feeding allows a more efficient infection of the abdominal region by *Y. pseudotuberculosis* without neck colonization compared to the needle feeding.

Fig. 6. Comparative analysis of the course of infection using the three protocols of administration with 2.5E7 CFU of *Y. pseudotuberculosis*.

OF1 mice were orally infected with 2.5E7 (A, B, C) *Y. pseudotuberculosis* strain IP32953-*lux* CFUs and monitored overtime for BLI signal, weight loss and mortality after needle feeding of bacteria resuspended in PBS (black line), in PBS supplemented with $CaCO_3$ (green line), or after bread feeding of bacteria resuspended in PBS only (red line).

Quantification of the bioluminescent signal from the abdominal region is shown below the mice pictures in each condition at each time point (24, 48, 72 and 168-192 h p.i.). Red dotted lines indicate the average radiance of ROI measurements above which animals are in terminal illness. Red crosses positioned on the X axis indicate dead mice. Comparative weight loss (B) and survival of mice (C) for 21 days using the three protocols of administration.

Fig. 7 Comparative analysis of animal survival after oral infection with *Y. pseudotuberculosis*.

OF1 mice survival after oral infection with serial dilutions of *Y. pseudotuberculosis* IP32953-*lux* using bread feeding (A), needle feeding supplemented with $CaCO_3$ (B) or needle feeding without $CaCO_3$ (C). Mice were observed daily and LD_{50} were determined according to the method of Reed and Muench (21).

Fig. 1

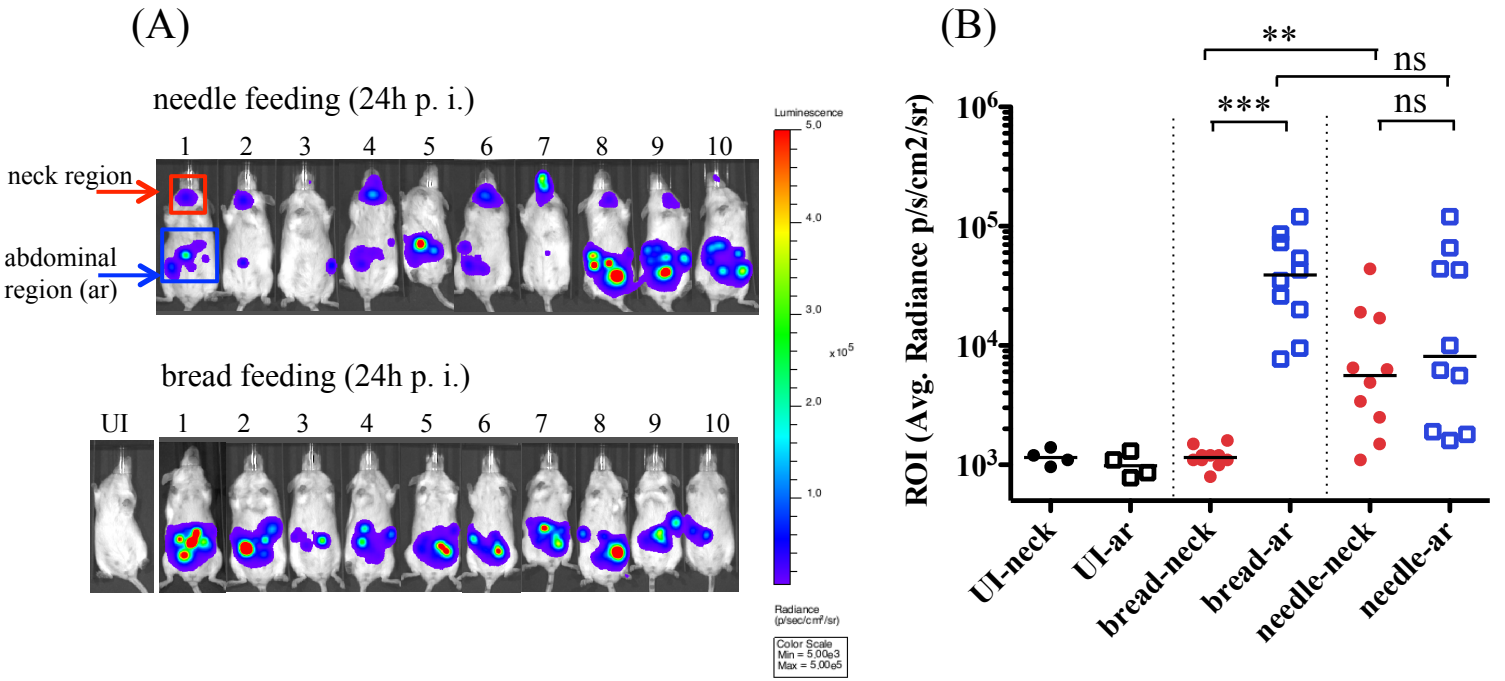
(A)
needle feeding (24h p. i.)
1 2 3 4 5 6 7 8 9 10
neck region
abdominal region (ar)
bread feeding (24h p. i.)
UI 1 2 3 4 5 6 7 8 9 10
Luminescence
5.0
4.0
3.0
x10^5
2.0
1.0
Radiance (p/sec/cm²/sr)
Color Scale
Min = 5.00e3
Max = 5.00e5
(B)
**
ns
***
ns
ROI (Avg. Radiance p/s/cm2/sr)
10^6
10^5
10^4
10^3
UI-neck
UI-ar
bread-neck
bread-ar
needle-neck
needle-ar

Fig. 2

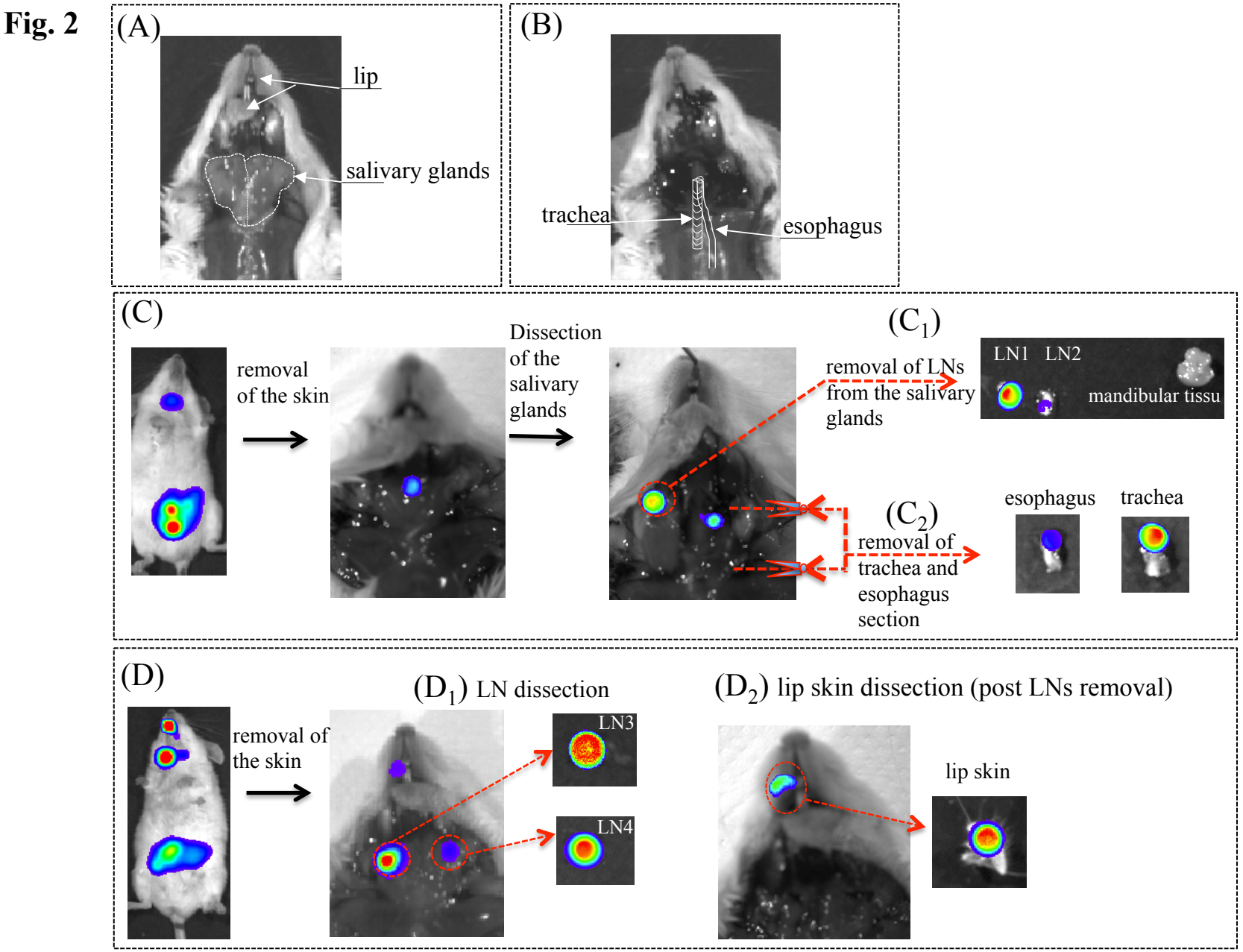
(A)
lip
salivary glands
(B)
trachea
esophagus
(C)
removal of the skin
Dissection of the salivary glands
(C1)
removal of LNs from the salivary glands
LN1
LN2
mandibular tissu
(C2)
removal of trachea and esophagus section
esophagus
trachea
(D)
removal of the skin
(D1) LN dissection
LN3
LN4
(D2) lip skin dissection (post LNs removal)
lip skin

Fig. 3

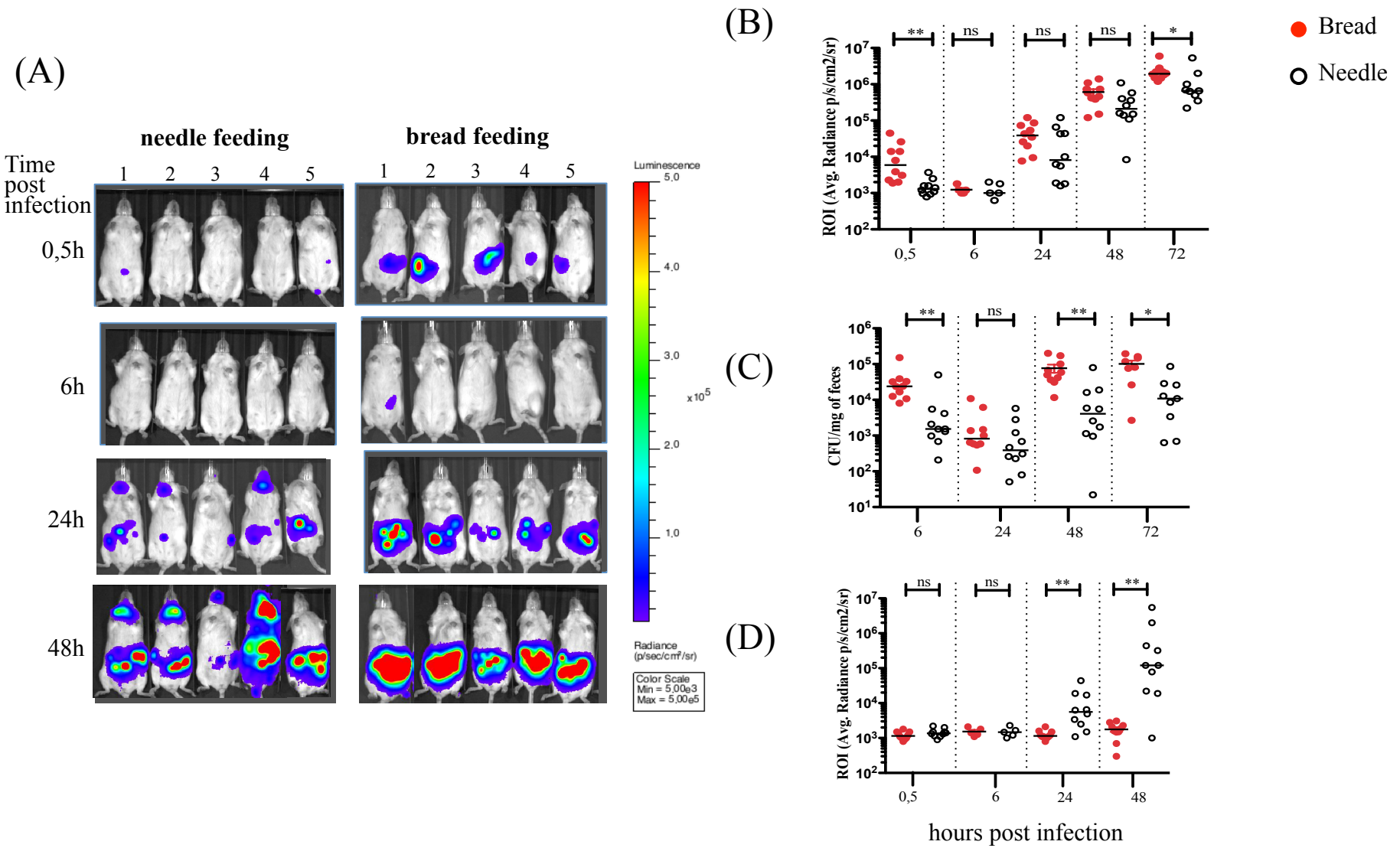
(A)
needle feeding
bread feeding
Time post infection
1 2 3 4 5
0,5h
6h
24h
48h
Luminescence
5,0
4,0
3,0
2,0
1,0
x10^5
Radiance (p/sec/cm²/sr)
Color Scale
Min = 5,00e3
Max = 5,00e5
(B)
ROI (Avg. Radiance p/s/cm2/sr)
**
ns
ns
ns
*
0,5
6
24
48
72
(C)
CFU/mg of feces
**
ns
**
*
6
24
48
72
(D)
ROI (Avg. Radiance p/s/cm2/sr)
ns
ns
**
**
0,5
6
24
48
hours post infection
Bread
Needle

Fig. 4

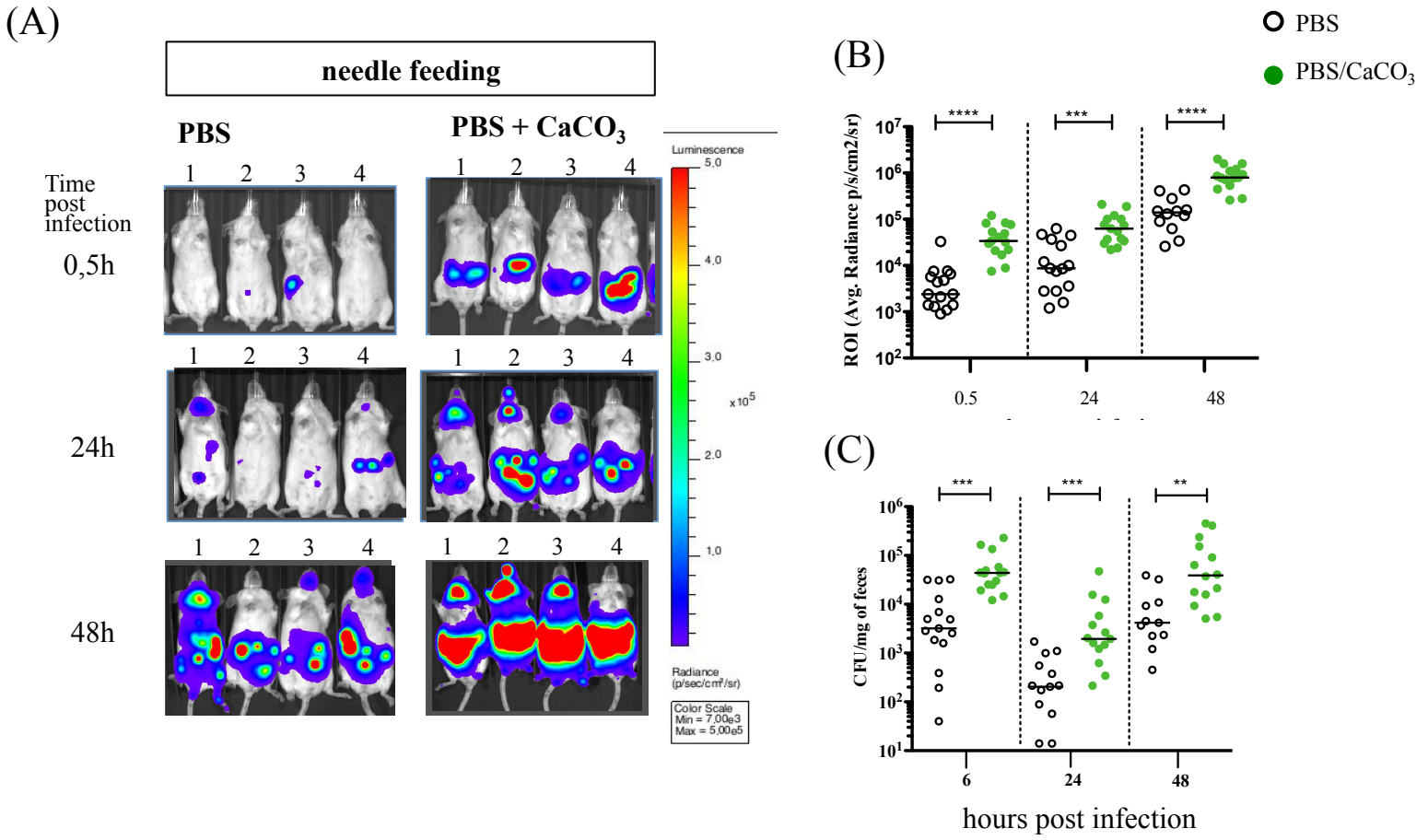
(A)
needle feeding
PBS
PBS + CaCO3
Time post infection
0,5h
24h
48h
1 2 3 4
Luminescence
5,0
4,0
3,0
x10^5
2,0
1,0
Radiance (p/sec/cm²/sr)
Color Scale
Min = 7,00e3
Max = 5,00e5
(B)
PBS
PBS/CaCO3
ROI (Avg. Radiance p/s/cm2/sr)
10^7
10^6
10^5
10^4
10^3
10^2
****
***
****
0.5
24
48
(C)
CFU/mg of feces
10^6
10^5
10^4
10^3
10^2
10^1
***
***
**
6
24
48
hours post infection

Fig. 5

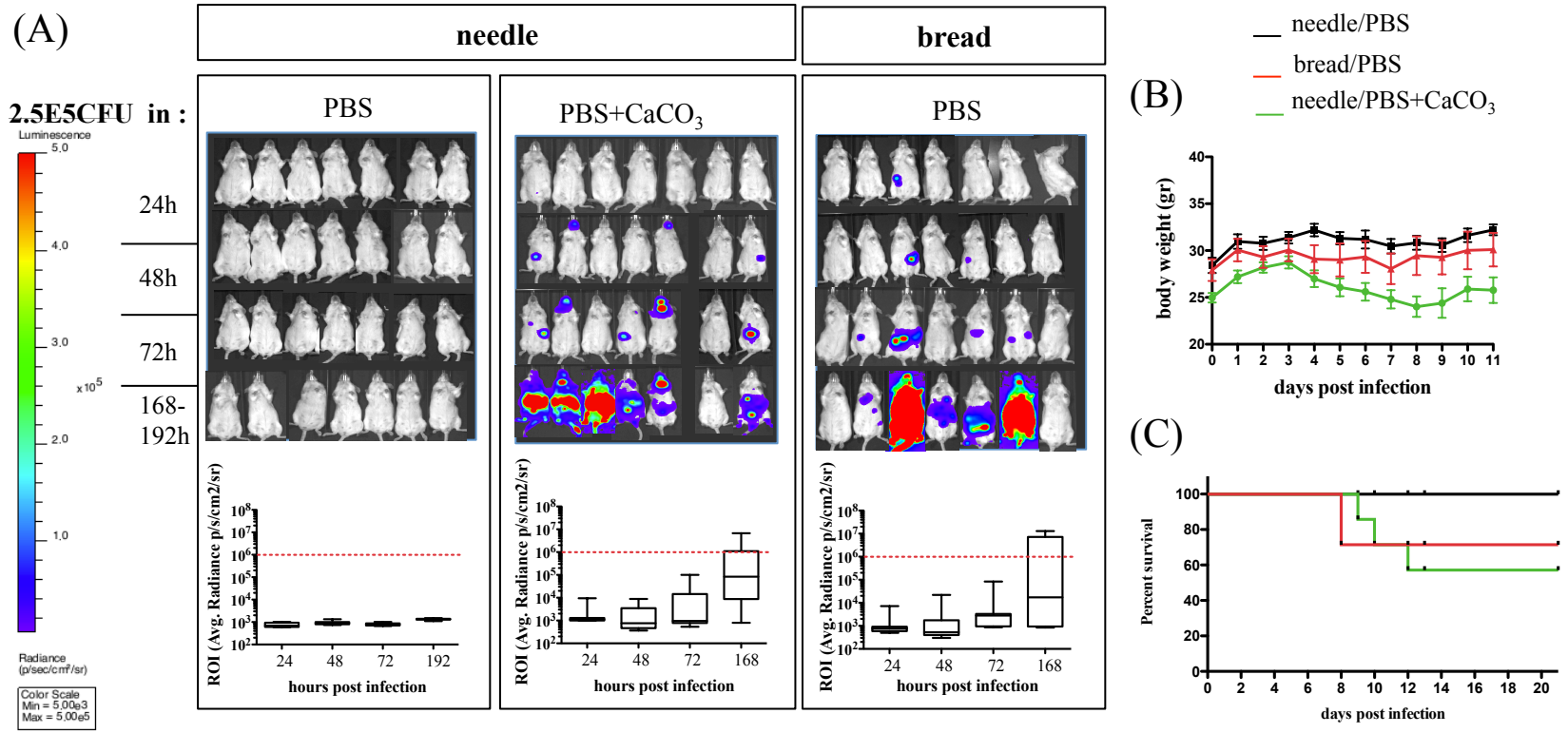
(A)
needle
bread
2.5E5CFU in :
PBS
PBS+CaCO3
PBS
24h
48h
72h
168-192h
Luminescence
Radiance (p/sec/cm²/sr)
Color Scale Min = 5,00e3 Max = 5,00e5
ROI (Avg. Radiance p/s/cm2/sr)
hours post infection
(B)
needle/PBS
bread/PBS
needle/PBS+CaCO3
body weight (gr)
days post infection
(C)
Percent survival
days post infection

Fig. 6

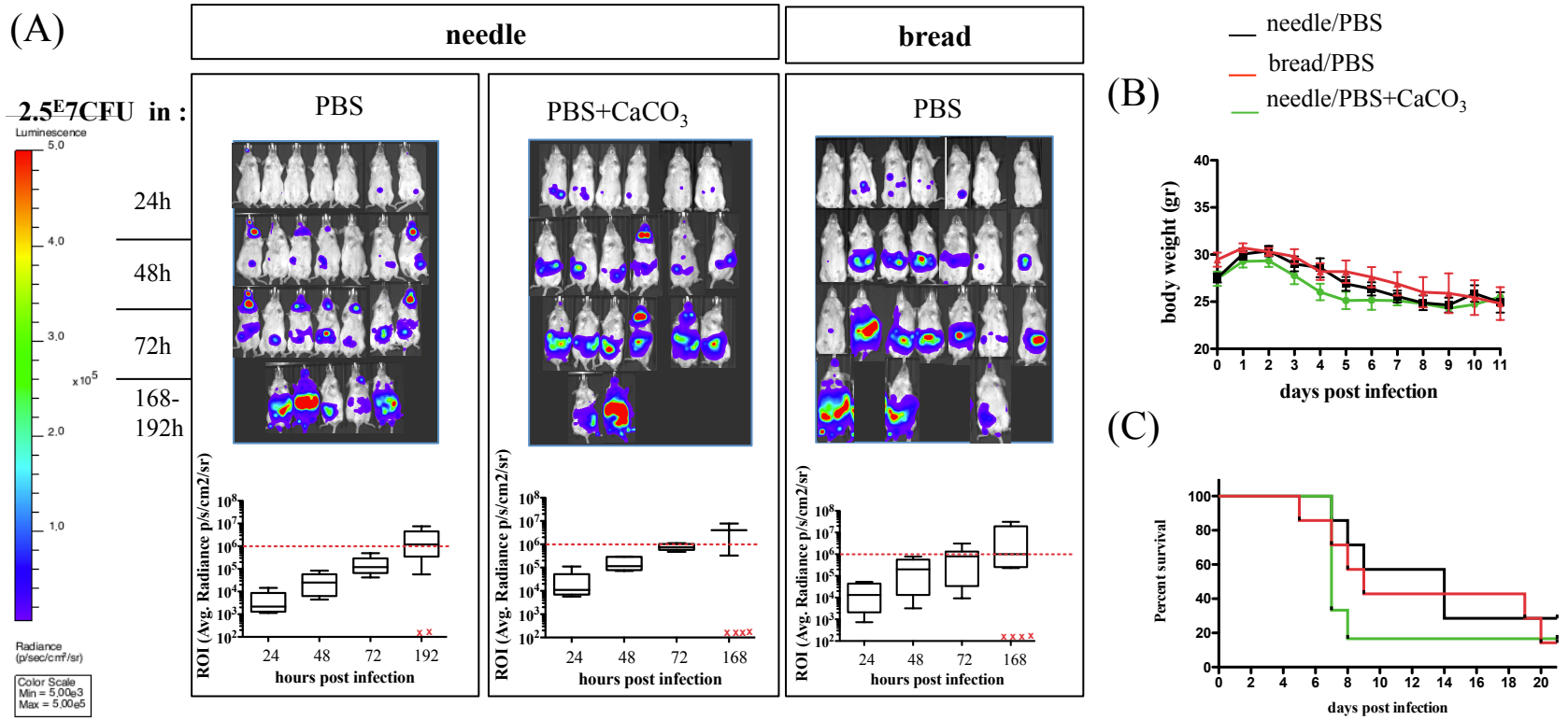
(A)
needle
bread
2.5E7CFU in :
PBS
PBS+CaCO3
PBS
24h
48h
72h
168-192h
Luminescence
Radiance (p/sec/cm²/sr)
Color Scale Min = 5,00e3 Max = 5,00e5
ROI (Avg. Radiance p/s/cm2/sr)
hours post infection
(B)
needle/PBS
bread/PBS
needle/PBS+CaCO3
body weight (gr)
days post infection
(C)
Percent survival
days post infection

Fig. 7

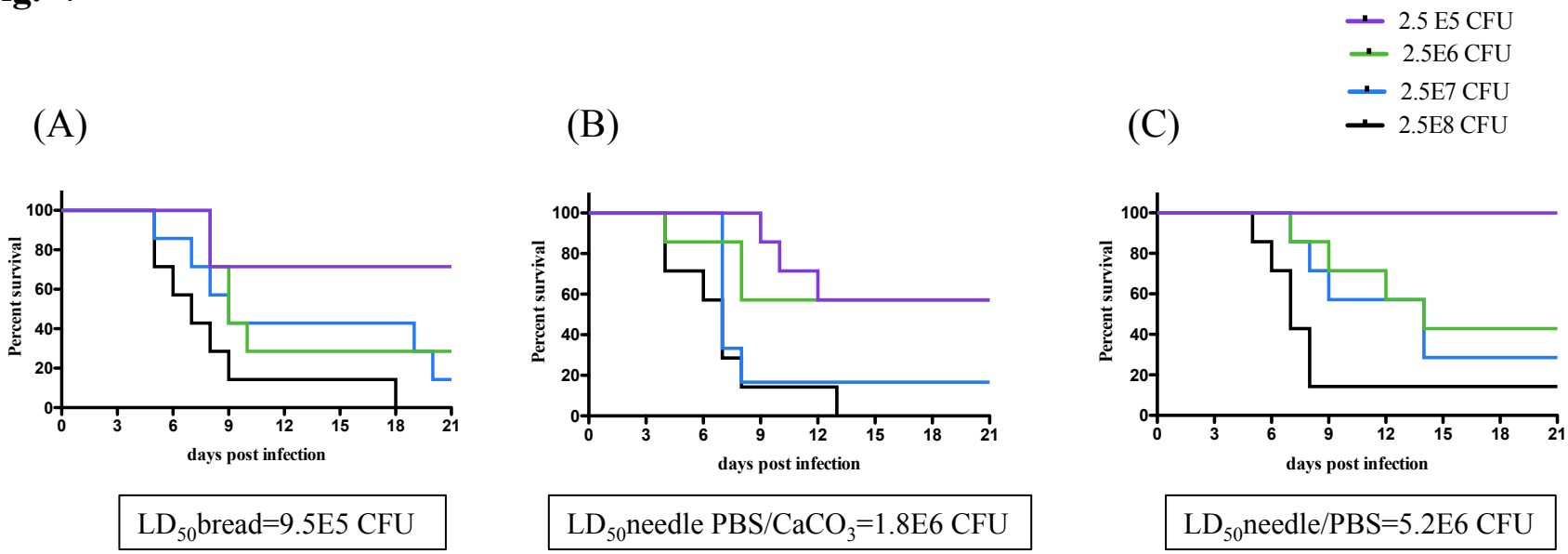
2.5 E5 CFU
2.5E6 CFU
2.5E7 CFU
2.5E8 CFU
(A)
(B)
(C)
Percent survival
days post infection
0
3
6
9
12
15
18
21
20
40
60
80
100
LD50bread=9.5E5 CFU
LD50needle PBS/CaCO3=1.8E6 CFU
LD50needle/PBS=5.2E6 CFU